APPENDIX A - FLAT PLATE, FALSE WALLS, AND NOZZLE VARIATIONS

During the course of the experiments, 14 different configurations of test plates and false walls were used. It is helpful to assign letters to each configuration tested, as well as each type of test plate and false wall. Table I lists each configuration with the type of test plate and false wall involved. Table II provides a short description of the features of each type of test plate and false wall.

Table II - Test Plate and False Wall Configurations.

Configuration	Plate	False Wall
A	A	None
B	B	None
C	C	None
D	C	A
E	C	B
F	D	A
G	D	None
H	C	C
I	D	C
J	D	None
K	D	D
L	E	D
M	E	E
N	E	F

Table III - Test Plate and False Wall Types

Plates

A Sharp leading edge and underside corner, no trailing edge fairing, 6 support rods without fairings.

B Sharp leading edge and underside corner, trailing edge fairing and 4 support rods with fairings.

C Sharp leading edge, clay on underside corner, trailing edge fairing and fairings on the four support rods.

D Leading edge blunted with clay, clay on underside corner, trailing edge fairing and fairings on the four support rods.

E New leading edge fairing with blunt design, new trailing edge fairing to contain new transducer and eliminate sharp corners, six support rods with fairings.

False Walls

A First single floor false wall design.

B Type A false wall with slight contour modification.

C Type A false wall with concavity eliminated.

D Twin false wall design with symmetrical false walls on wind tunnel test section ceiling and floor.

E Same as type D, but with floor false wall removed.

F As in type D with fillet blocks near front of ceiling false wall and an obstruction block added to aft portion of ceiling false wall.

Three flow quality areas governed design of the test plate system: pressure gradient along the plate, attached flow on the plate leading edge, and minimization of the interference from the particle injection nozzle. This is a short history of the plate and nozzle design development. The primary area of concern was the pressure gradient, and the other items became more important as the designs evolved.

The original plate configuration, plate A, is shown in Figure 38. Figure 39 shows the uncorrected pressure gradient over plate system A (configuration A). In this configuration an abrupt acceleration of flow occurs at the wedge-shaped leading edge, followed by an equally rapid deceleration. Fifteen inches downstream from the leading edge, the boundary layer growth along the plate and tunnel walls again accelerates the flow.

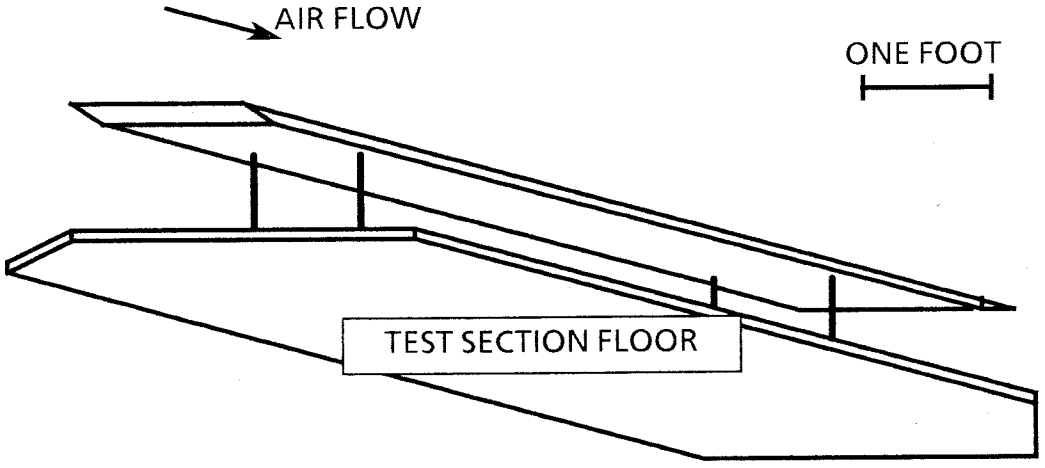

Figure 38. - Plate configuration A

Of the test plates, plate B had the first aerodynamic treatment of any consequence, featuring a $3\frac{1}{2}$ inch long trailing edge fairing and fairings on the support rods to reduce dynamic pressure loss (and static pressure increase) along the tunnel test section. Plate B is illustrated in Figure 40. Unfortunately, separation was caused on the lower corner of this plate due to a sharp corner at the lower leading edge. This was eliminated by smoothing the corner with clay, as shown in Figure 41. Flow visualization provided by injection of particles over the plate gave the initial indication of separation, and also showed the attached flow with the clay. This treatment distinguishes plate B from plate

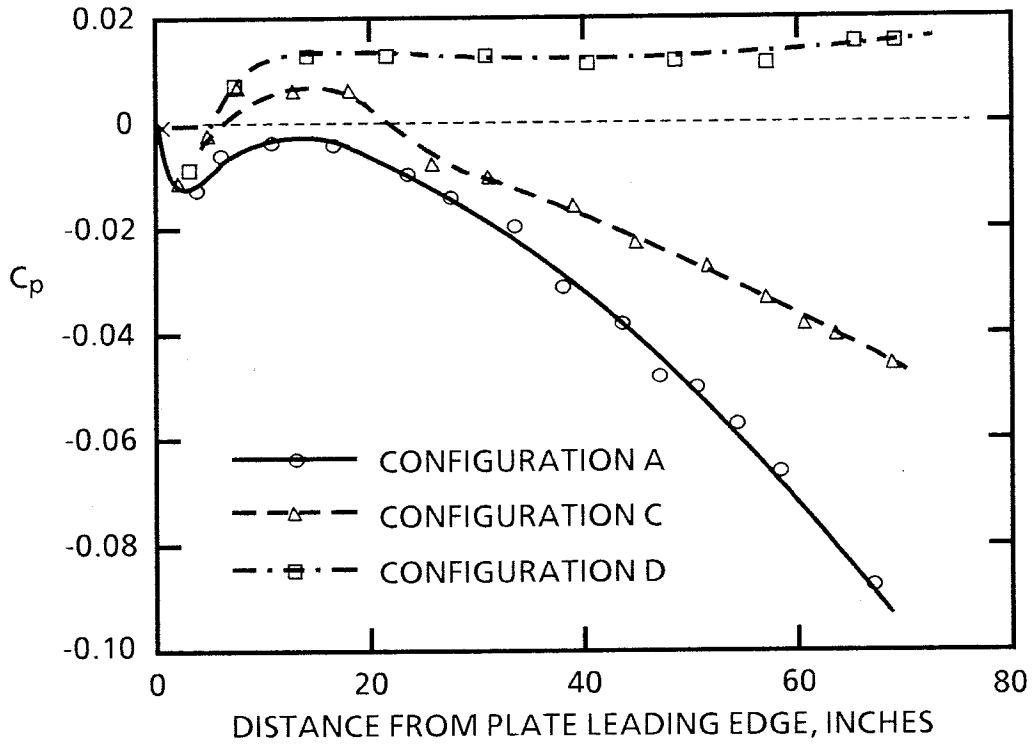

Figure 39 - Pressure distribution of configurations A, C, and D.

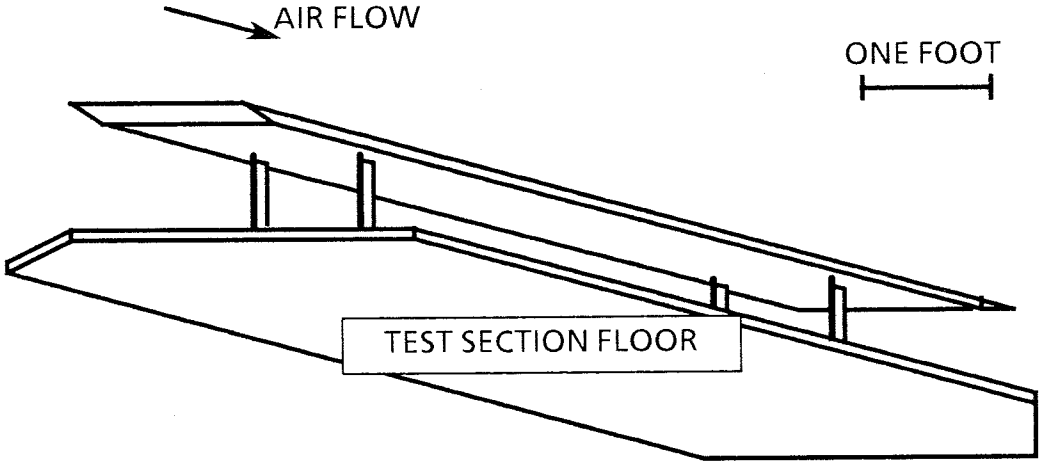

Figure 40 - Scale oblique view of plate B.

C. Although the acceleration of flow over the aft portion of the plate was alleviated, little over-all smoothing of the pressure distribution resulted.

A false wall was designed which was located underneath the plate system. In order to avoid the problems caused by slight surface ripple on wide false walls as experienced by

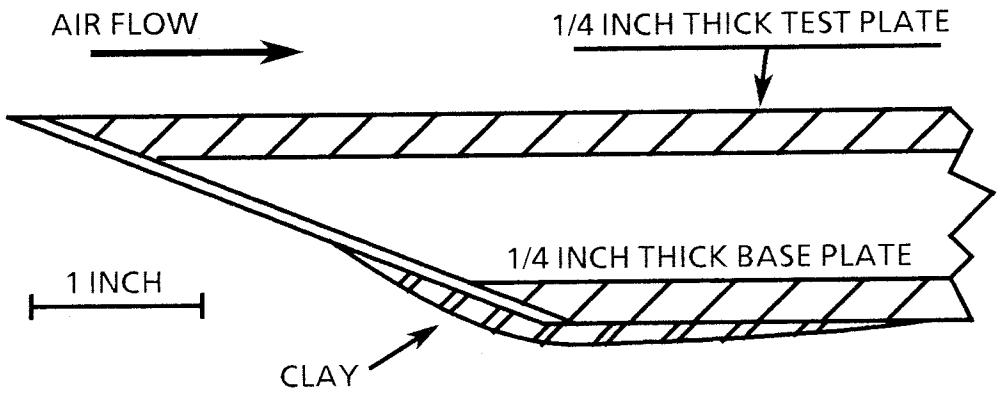

Figure 41 - Plate C leading edge detail, cross section side view.

Klebanoff and Deihl[41], the model A false wall was designed fairly thick and only a foot wide to fit in the available floor space. This had a profile determined from pressure measurements along the plate. The profile coordinates are listed in Table III. Use of this false wall and plate C is designated configuration D, and is illustrated in Figure 42. This configuration proved to be quite successful in controlling the pressure gradient.

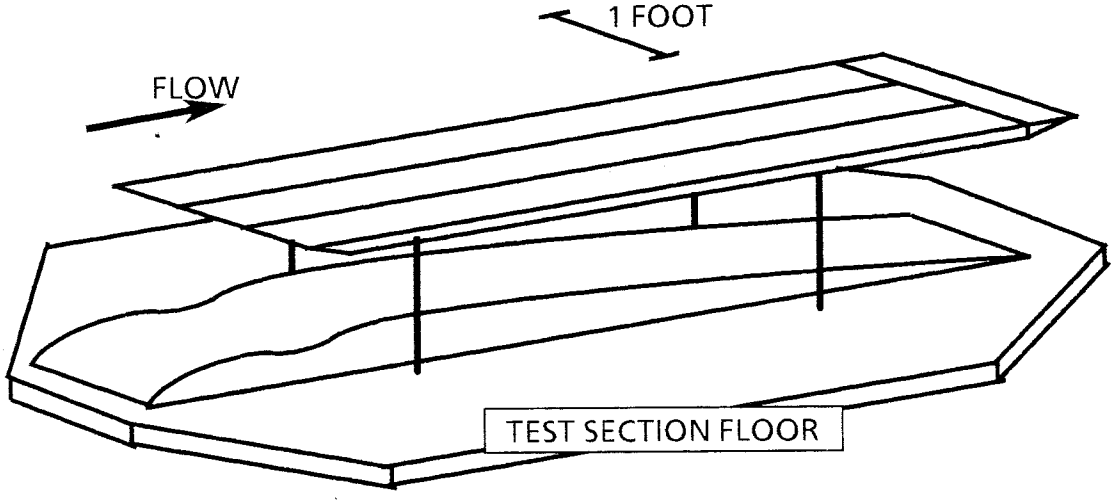

Figure 42 - False wall A with plate B shown for reference, oblique view.

Although a satisfactory pressure gradient was produced along the test plate, flow conditions were not acceptable. Separation was apparent at the upper leading edge of the plate. Contour modifications of the test plate as shown in Figure 43 did not correct the problem. False wall type B and C resulted from the contour modifications. These had

Table IV - Profile Coordinates of False Wall 'A'

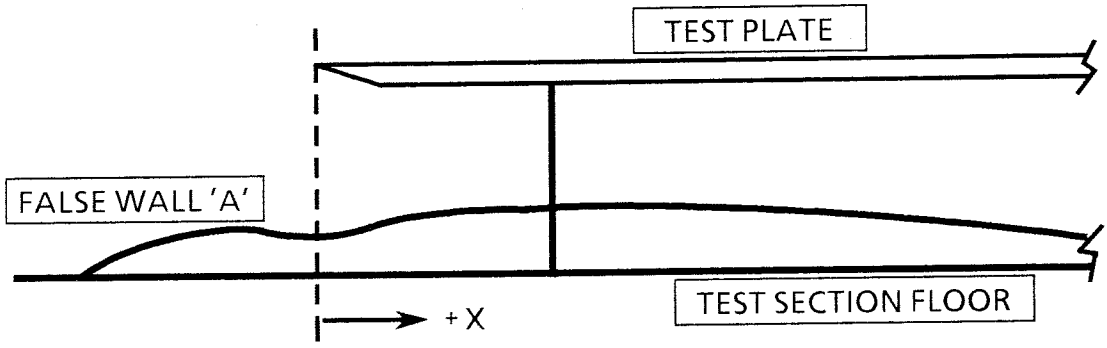

X, INCHES	FALSE WALL THICKNESS, INCHES
0.00	2.92
2.25	2.70
5.00	2.76
7.75	3.30
12.50	3.38
18.50	3.10
26.00	2.76
31.50	2.30
39.00	1.98
45.25	1.51
52.25	1.27
57.25	0.86
61.00	0.54
64.50	0.37
69.25	0.00

the concave portion of the false wall underneath the leading edge of the plate system filled in to various degrees to promote local flow acceleration and attachment. In Figure 44 the pressure distribution resulting from the type B false wall (configuration E) can be

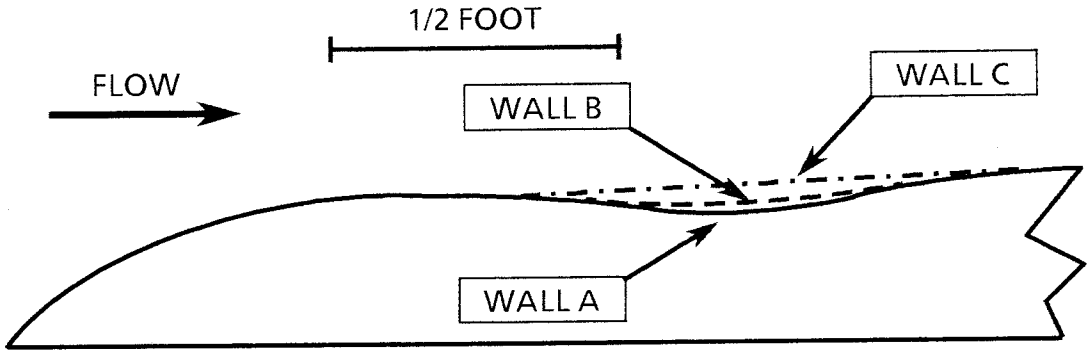

Figure 43 - Single false wall contour modifications

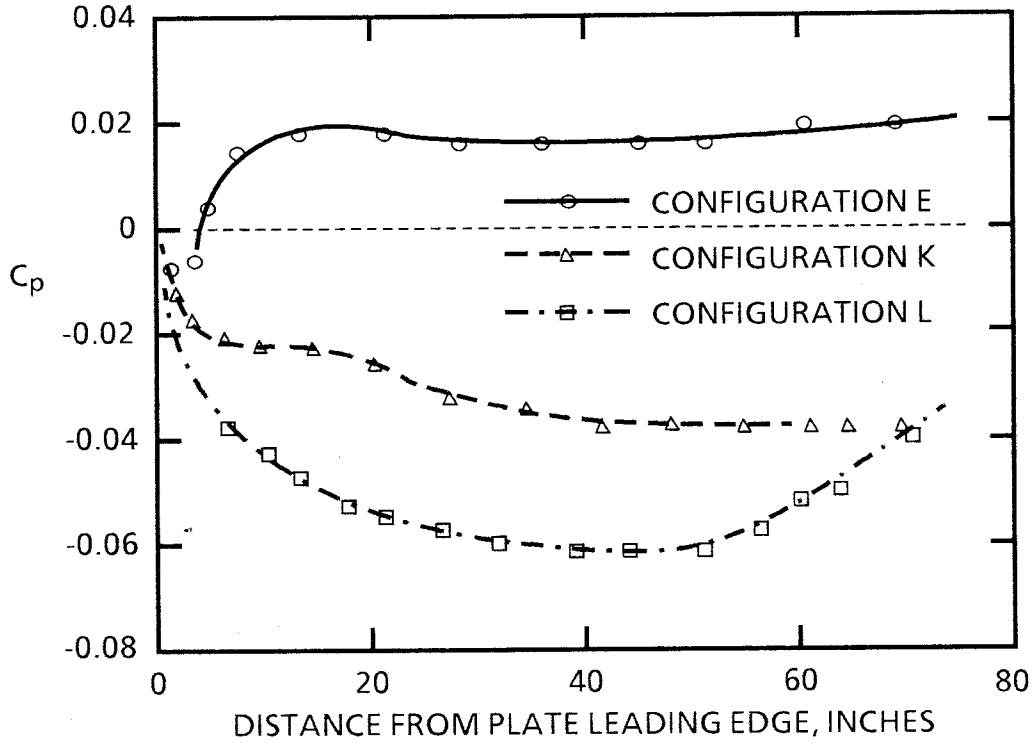

Figure 44 - Pressure distribution of plate configurations E, K, and L.

seen, which approximately the same as false wall type C. Both modifications had little effect on separation.

Boundary layer measurements revealed that separation occurred on this plate system design. In Figure 45, boundary layer profiles are shown from configuration E, taken along the plate centerline. This plate system had a very sharp leading edge, which

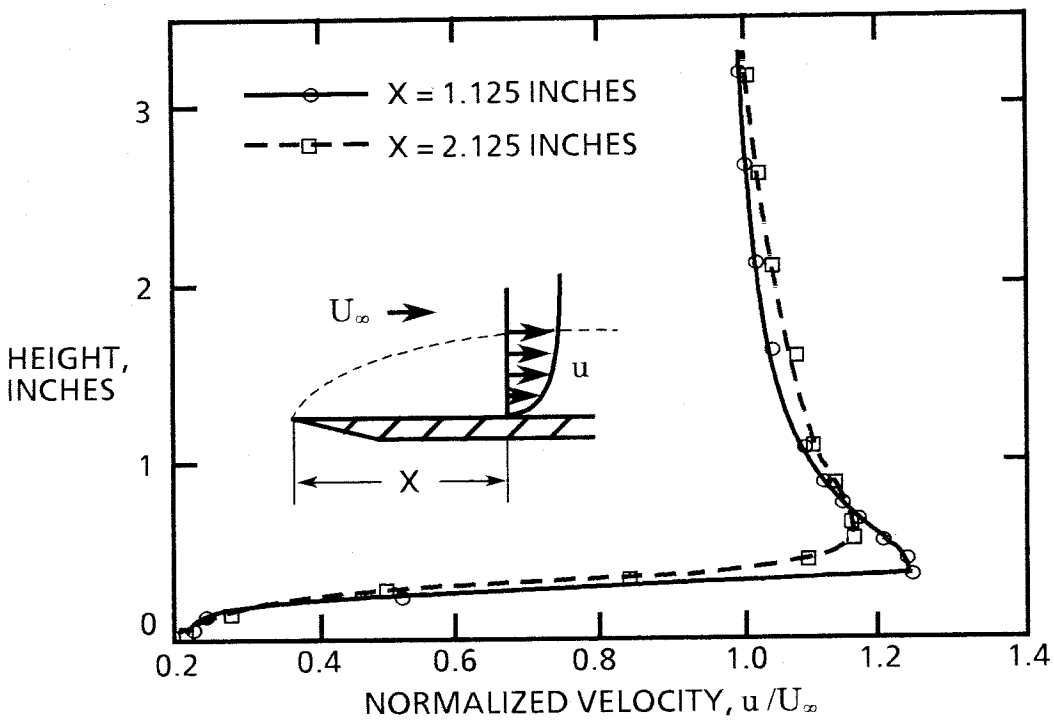

Figure 45(a) - Velocity profiles of configuration E.

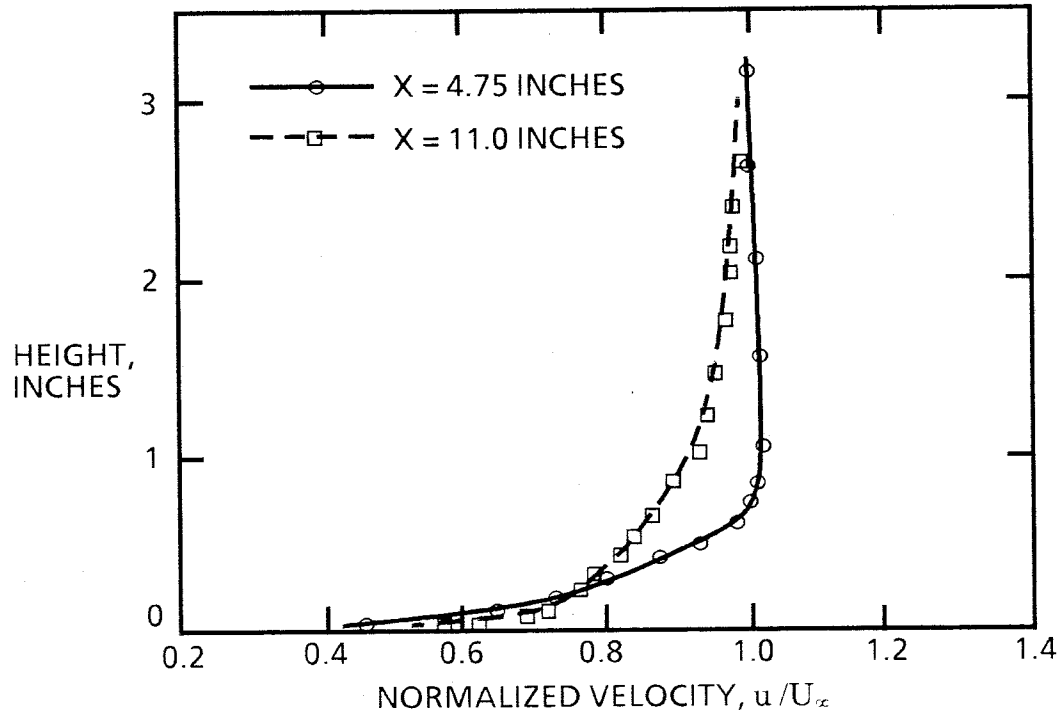

Figure 45(b) - Velocity profiles of configuration E.

clearly did not provide stable flow attachment without separation. The flow acceleration region is typical of large bubble laminar boundary layer separation, with the sharp velocity gradient at the fluid interface to the vortex. Since the flow is highly unsteady and the hot-wire does not sense direction of flow, the readings near the plate surface in strong separation regions are not reliable.

Blunting or rounding of the sharp leading edge on the test plate was investigated as a means to alleviate separation. This modification is called plate D, which had clay applied as shown in Figure 46. Progressive improvements with leading edge bluntness,

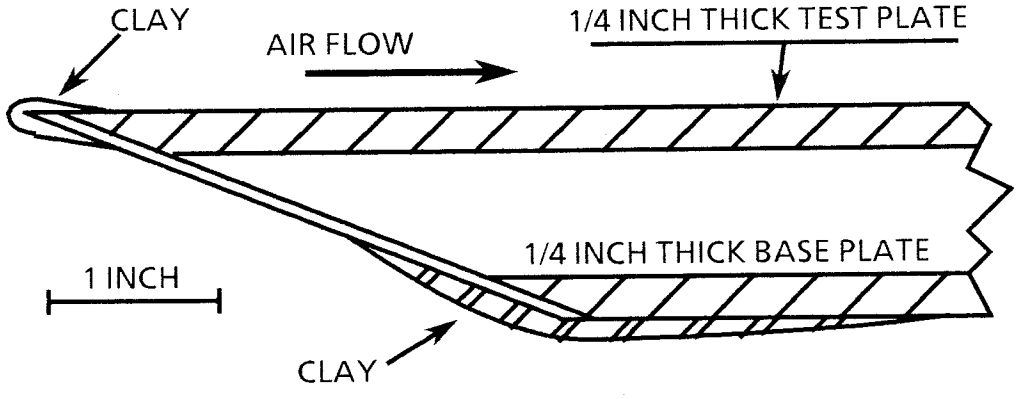

Figure 46 - Leading edge blunting experiment (plate D)

and the elimination of the asymmetric false wall, as shown in Figure 47, encouraged an entirely new false wall and leading edge design. This was studied after the influence of the false wall was better understood.

It was apparent that another factor contributing to separation on the plate was a flow disturbance caused by the false wall underneath the test plate. To reduce the flow disturbance false wall D was contructed, which was a symmetrical false wall. One false wall was located above the test plate, and one below. Each false wall was one foot wide, with a thickness half that of false wall A at equal longitudinal stations. In configuration K with the model D plate system and model D false wall, a reasonable pressure

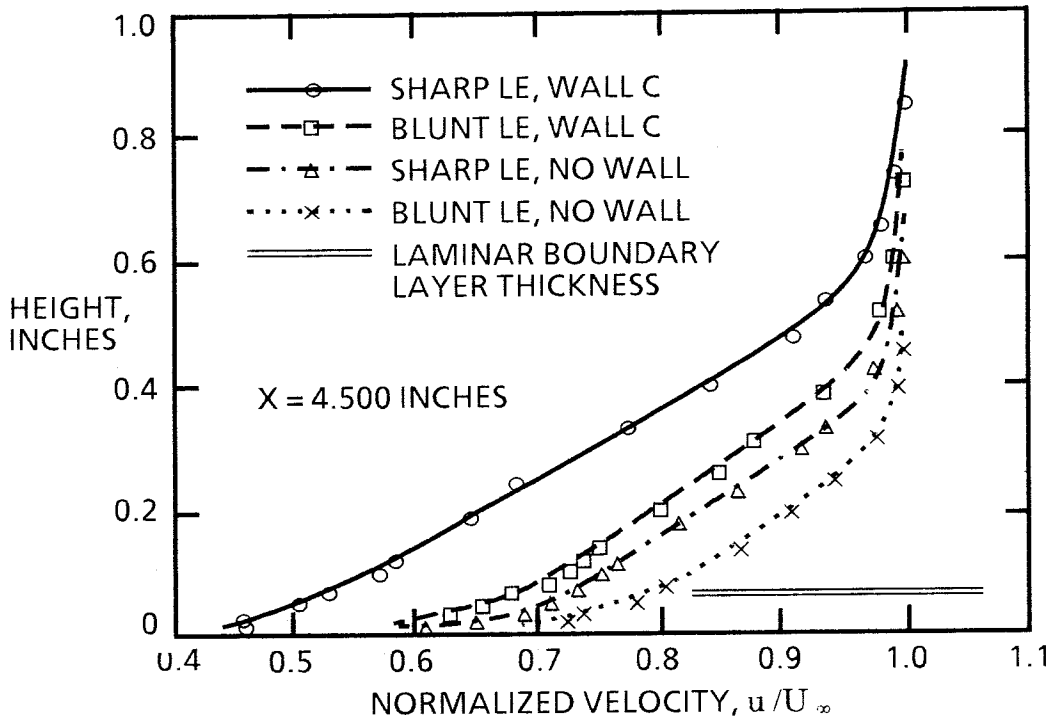

Figure 47 - Effects of wall and leading edge modifications

distribution resulted, as shown in Figure 44. The twin false walls do not promote leading edge separation. This is proven in Figure 48, where it is shown that velocity profiles with and without the twin false walls are approximately the same.

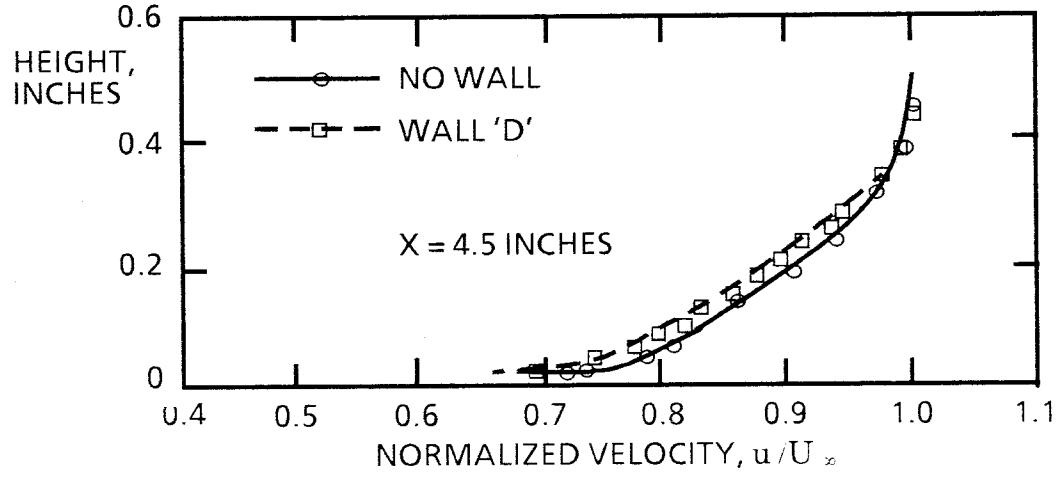

Figure 48 - Effect of twin false wall configuration

The success of leading edge bluntness in reducing and eliminating separation resulted in an entirely new leading and trailing edge profile to the test plate (see Figure 49). The new leading edge was based on the parametric geometry determined by Davis.The addition of the leading edge fairing extended the leading edge seven and one-

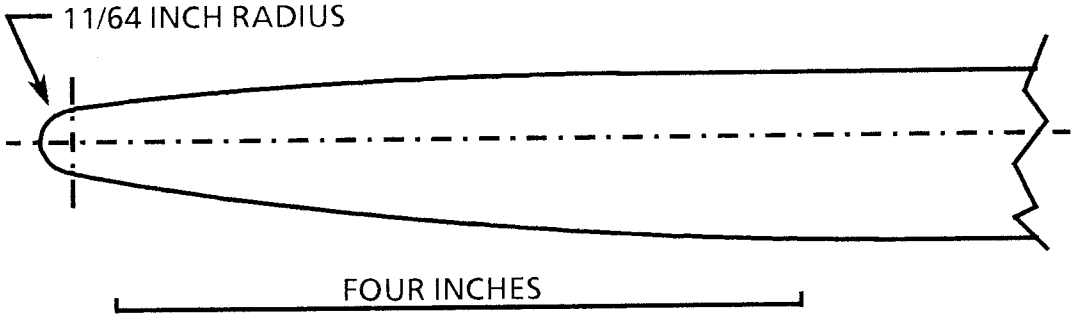

Figure 49 - Type E plate system leading edge fairing contour

quarter inches forward of the front edge of the test plate. This also prevented leading-edge pressure disturbances from affecting the test plate. A general view of the plate system is shown in Figure 50. Although the variation of pressure along the test plate is much larger than in earlier configurations, it almost meets the criteria derived from Klebanoff and Diehl. The choice of the leading edge as a reference point facilitates the

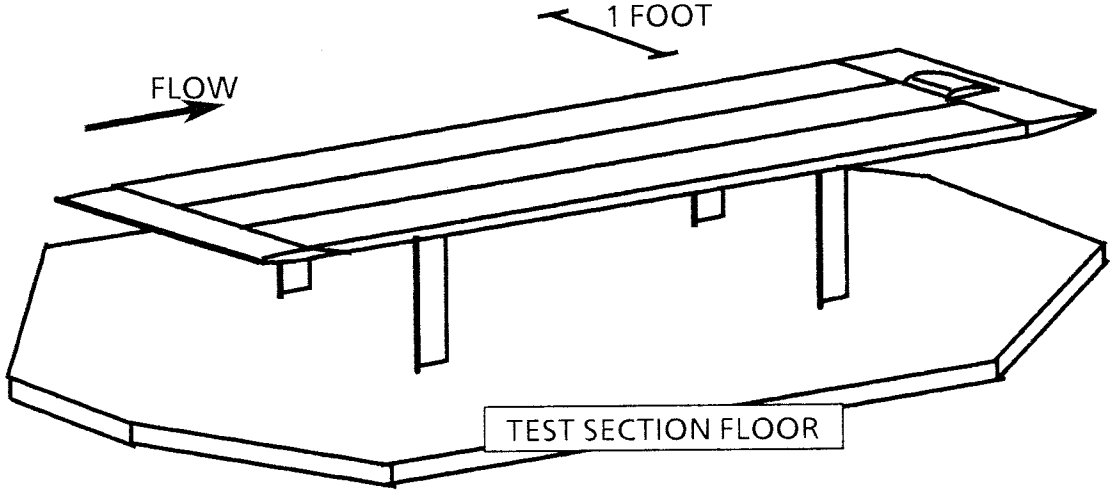

Figure 50 - Plate system with special leading and trailing edge fairings, plate E

comparison of the later type plate system with earlier ones. The locations of the false walls relative to the test plate are shown in Figure 51. A comparison with the Blasius laminar boundary layer theory prediction of boundary layer thickness can be seen in Figure 52.

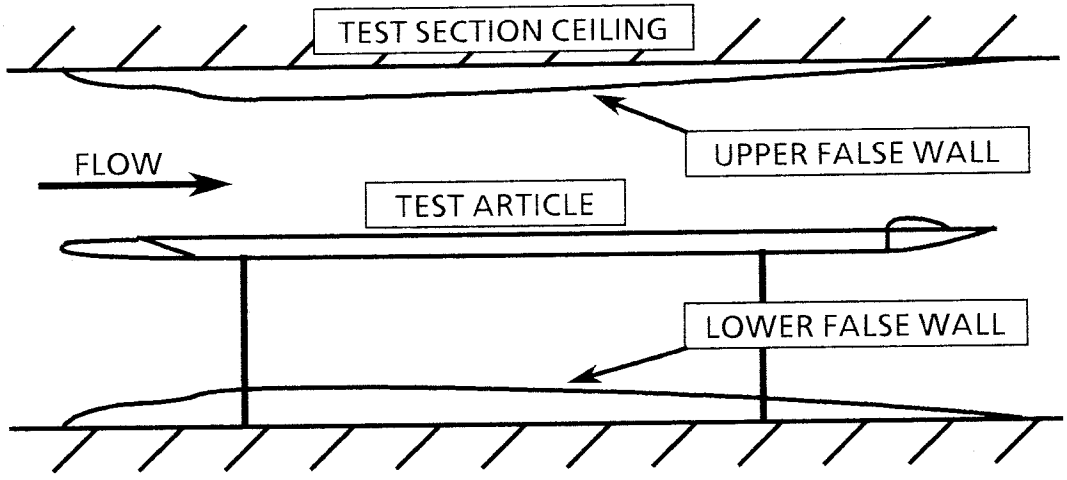

Figure 51 Twin false wall configuration, false wall D, configuration L.

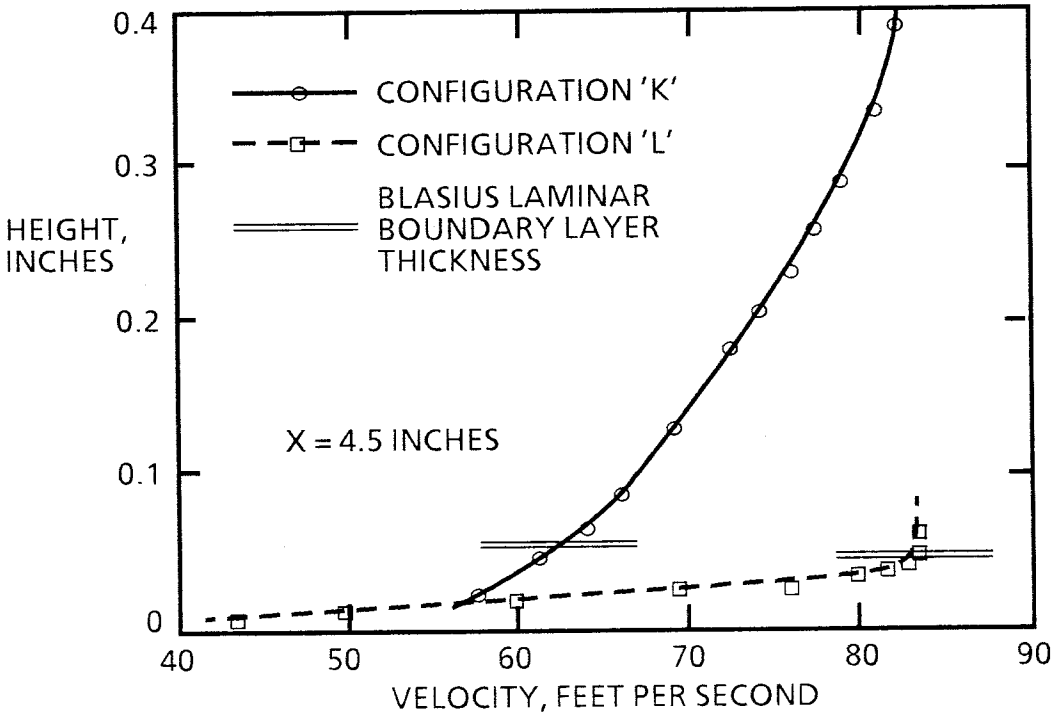

Figure 52 Comparison with laminar boundary layer thickness

With the separation on the test plate eliminated, efforts were made to correct the pressure gradient arising from the changes to the test plate. The floor false wall of false wall D was removed, and this configuration is called configuration type M. It produced a pressure distribution as in Figure 53, which was still unacceptable. Finally two side fillets and an obstruction block were added to the upper false wall of false wall D to give the type F false wall configuration of Figure 54.

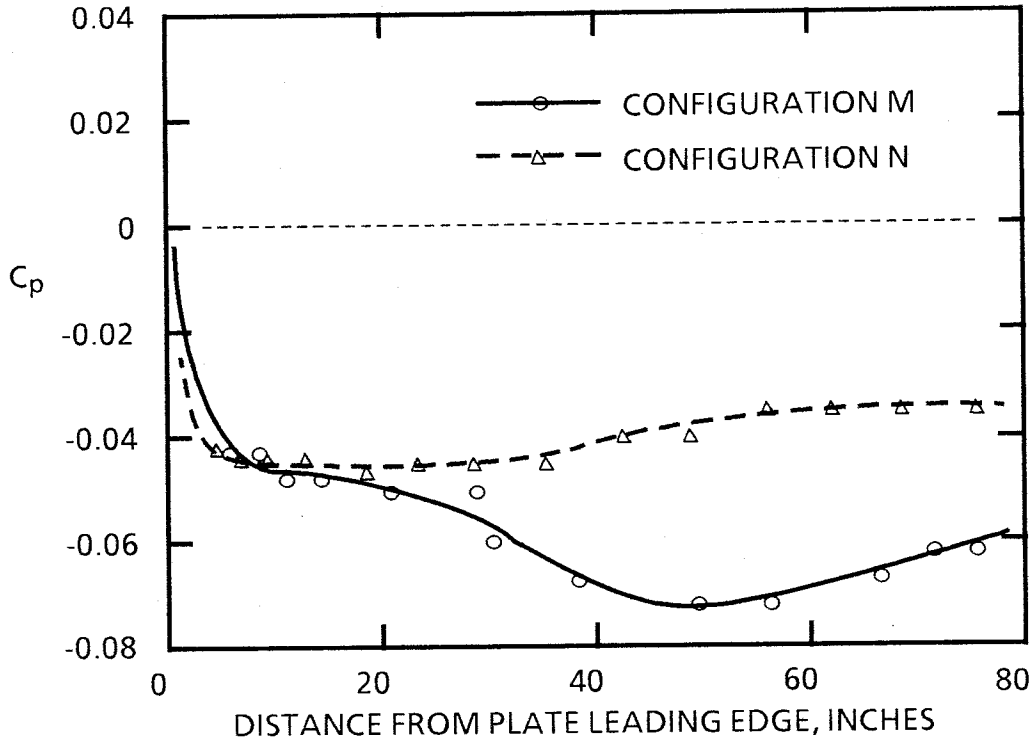

Figure 53 - Pressure distribution of configurations M and N.

Two different particle injection nozzle installations were used during the test. As the best location of the nozzle for injecting particles into the flow over the center of the test plate could not be determined without testing, an adjustable nozzle was installed (Figure 55). The cable and pulley arrangement allowed movement of the nozzle while the wind tunnel was running to acheive optimum injection of the particles. As shown in Figure 56, this system, with the nozzle end roughened by a helical coil of braided wire on

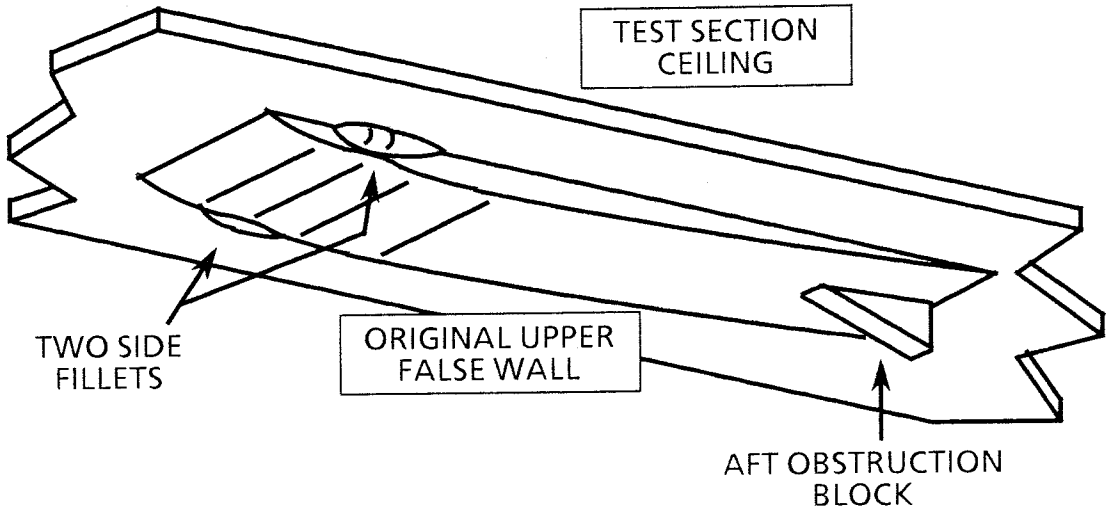

Figure 54 - Ceiling false wall with pressure gradient trim blocks, wall F

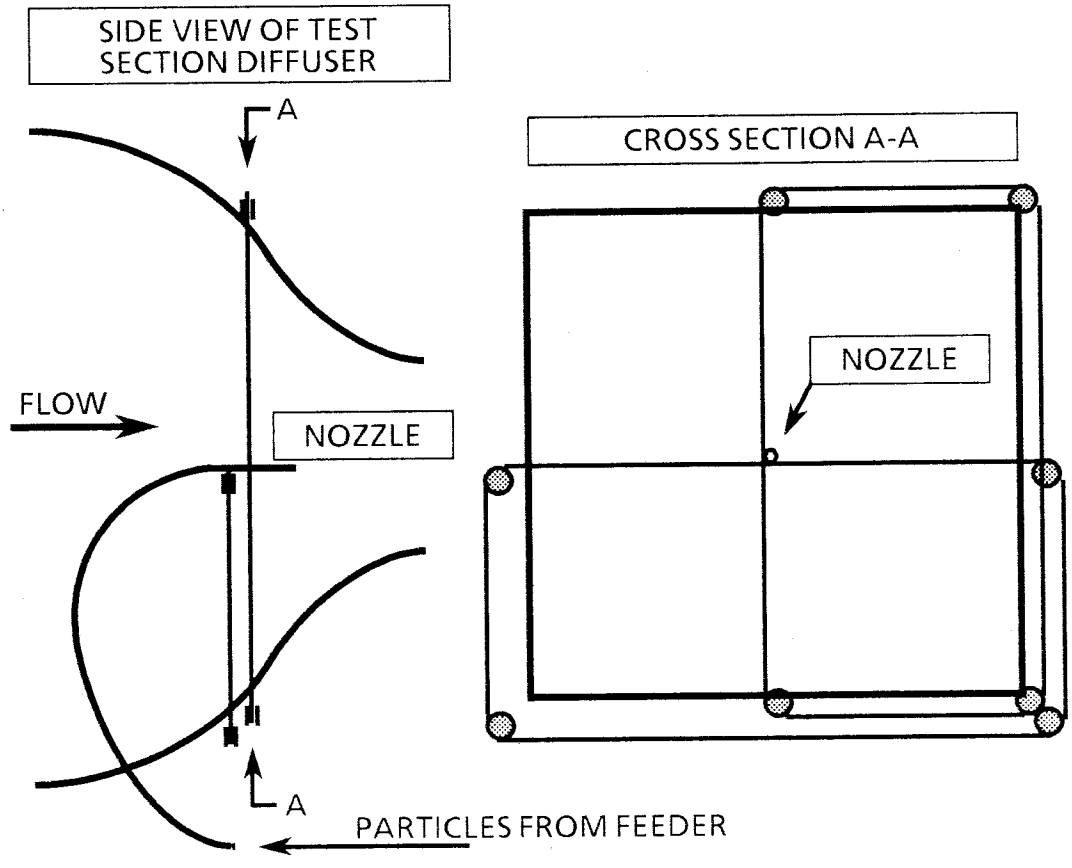

Figure 55 - Cable and pulley particle injector mounting.

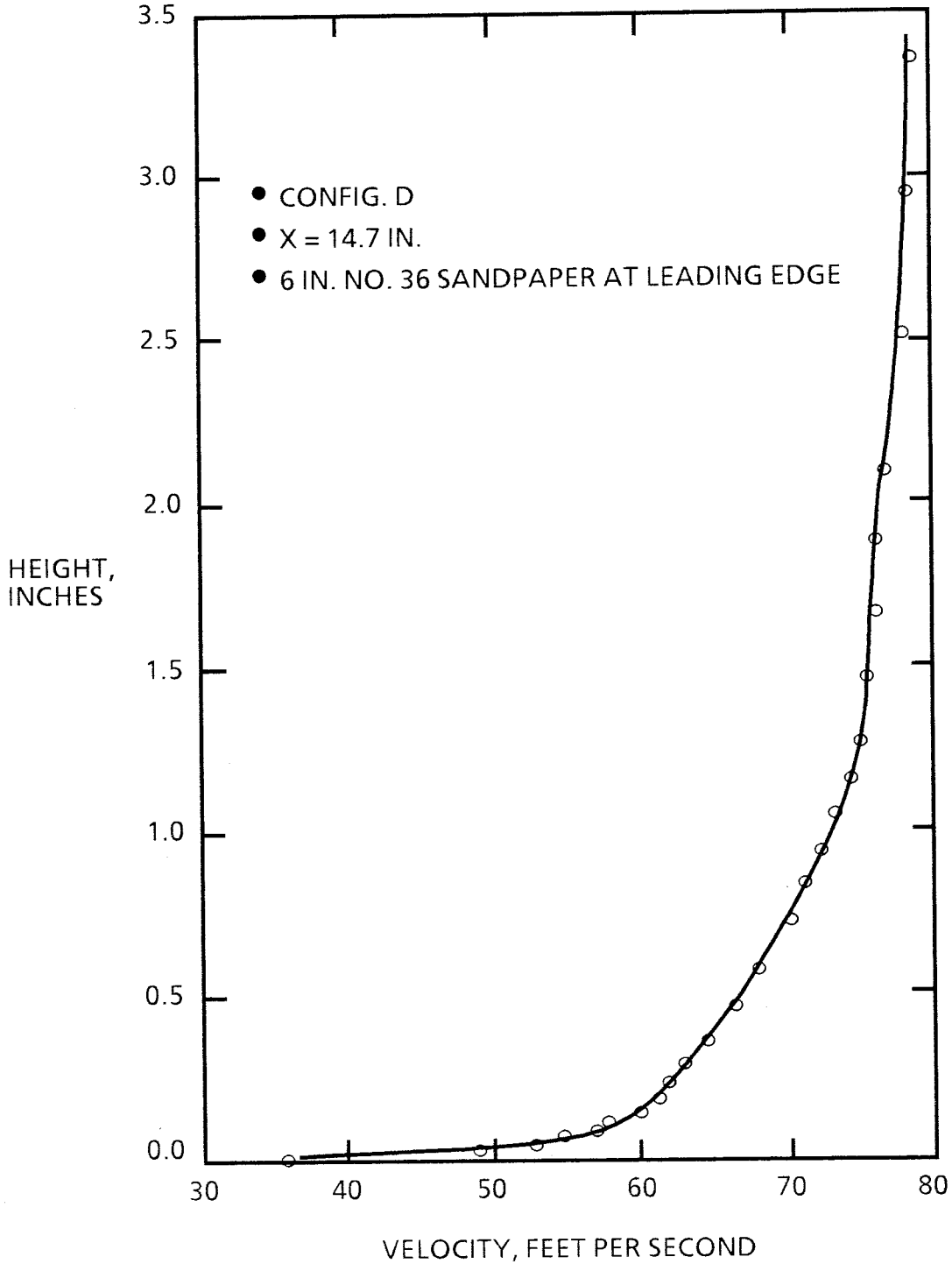

Figure 56 - Nozzle wake distortion of boundary layer

its outside surface, created a strong wake and severe distortion of the boundary layer some distance down the test plate.

The outside surface of the nozzle was smoothed, and the nozzle was moved to a distance of four feet from the leading edge of the plate system. In this configuration a test of the flow field three-eighths of an inch in front of the plate system leading edge could not reveal any velocity deficit from the wake of the nozzle, although the turbulent wake was detected as shown in Figure 57. It was shown that the nozzle produced a peak

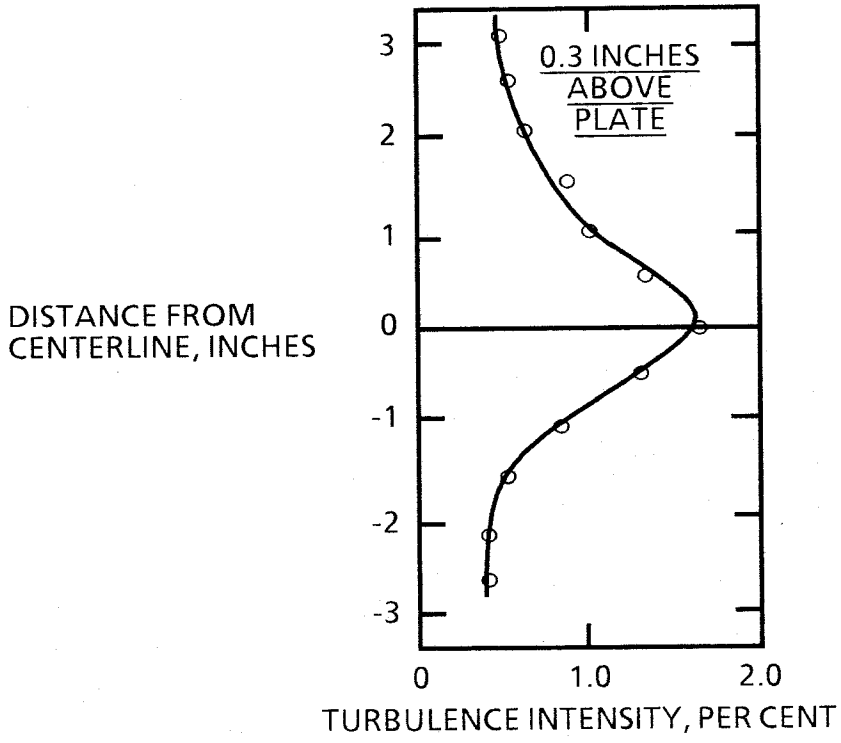

Figure 57(a) - Turbulence intensity three-eighths inch before plate system leading edge

turbulence intensity of about 1.5% near the center line of the plate. A strong turbulent wake was also produced by the support wires as seen in Figure 36(b), on the order of 0.5% to 1.0% in turbulence intensity.

In order to totally eliminate the wire wakes the support system was converted to a strut from the floor of the tunnel diffuser, once the optimum location of the nozzle was found (Figure 58). In this manner the wake from the strut passed underneath the plate

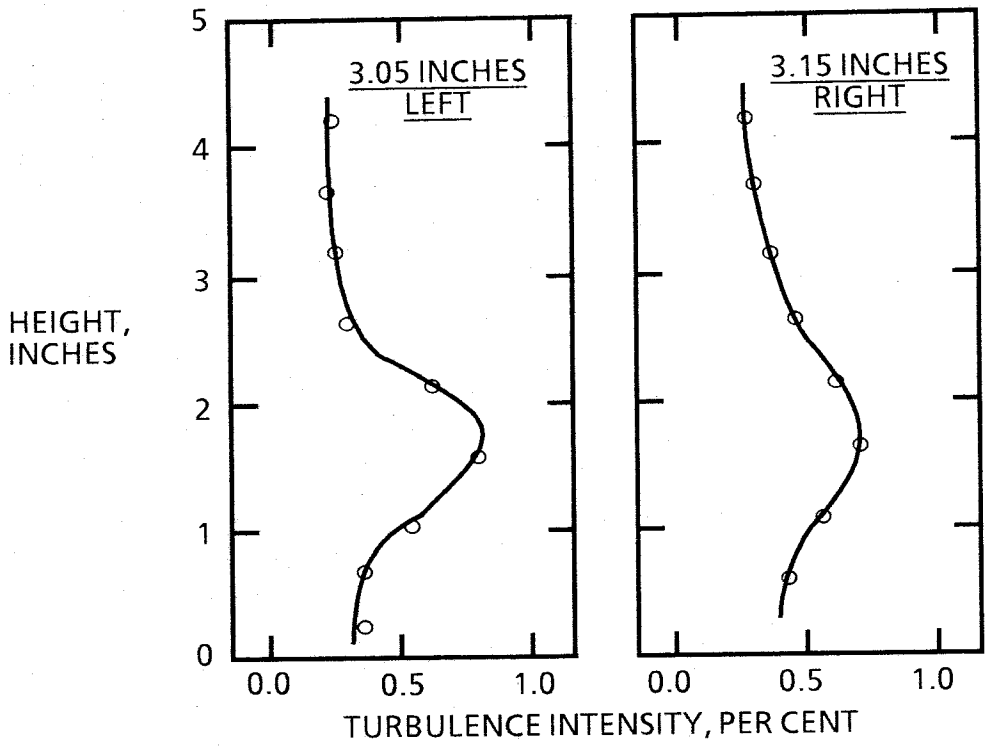

Figure 57(b) - Turbulence intensity three-eighths inch before plate system leading edge

system. By imposing a small upward angle to the injection nozzle, the particle stream travels upward before coming in equilibrium with the air stream and flowing over the test plate. The upward angle also allows the nozzle to be placed such that its wake passes below the plate system for the most part, as shown in Figure 59. In this test the free-stream turbulence intensity two-tenths inch above the plate is on the order of 1.1%, with turbulence quickly falling to moderate intensities an inch above the plate. It should be noted that this was measured in test configuration M, and the nozzle was located three feet, ten and one-half inches from the leading edge fairing.

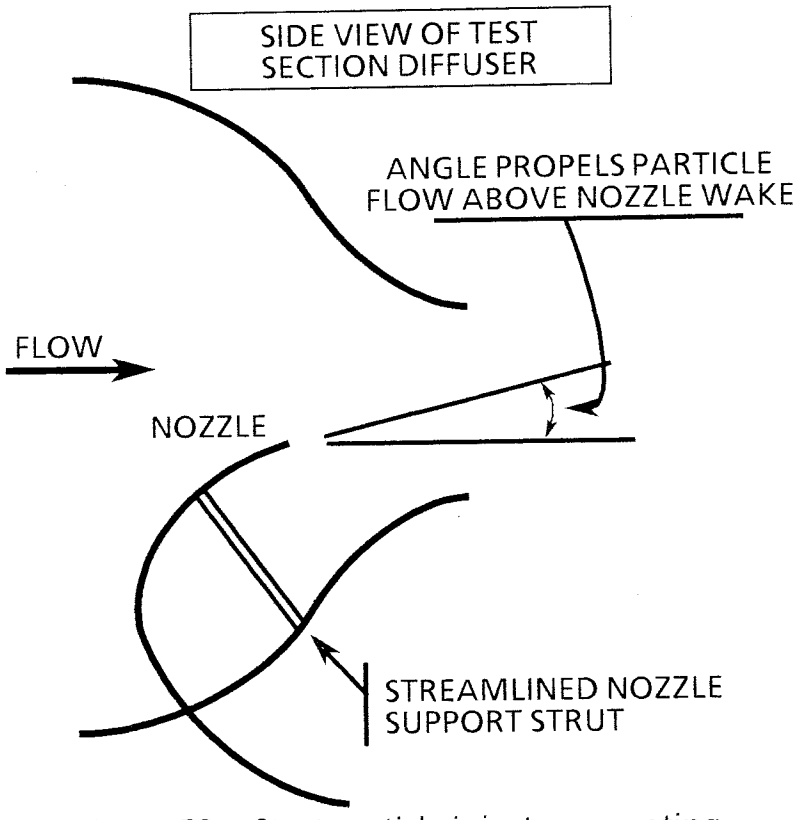

Figure 58 - Strut particle injector mounting.

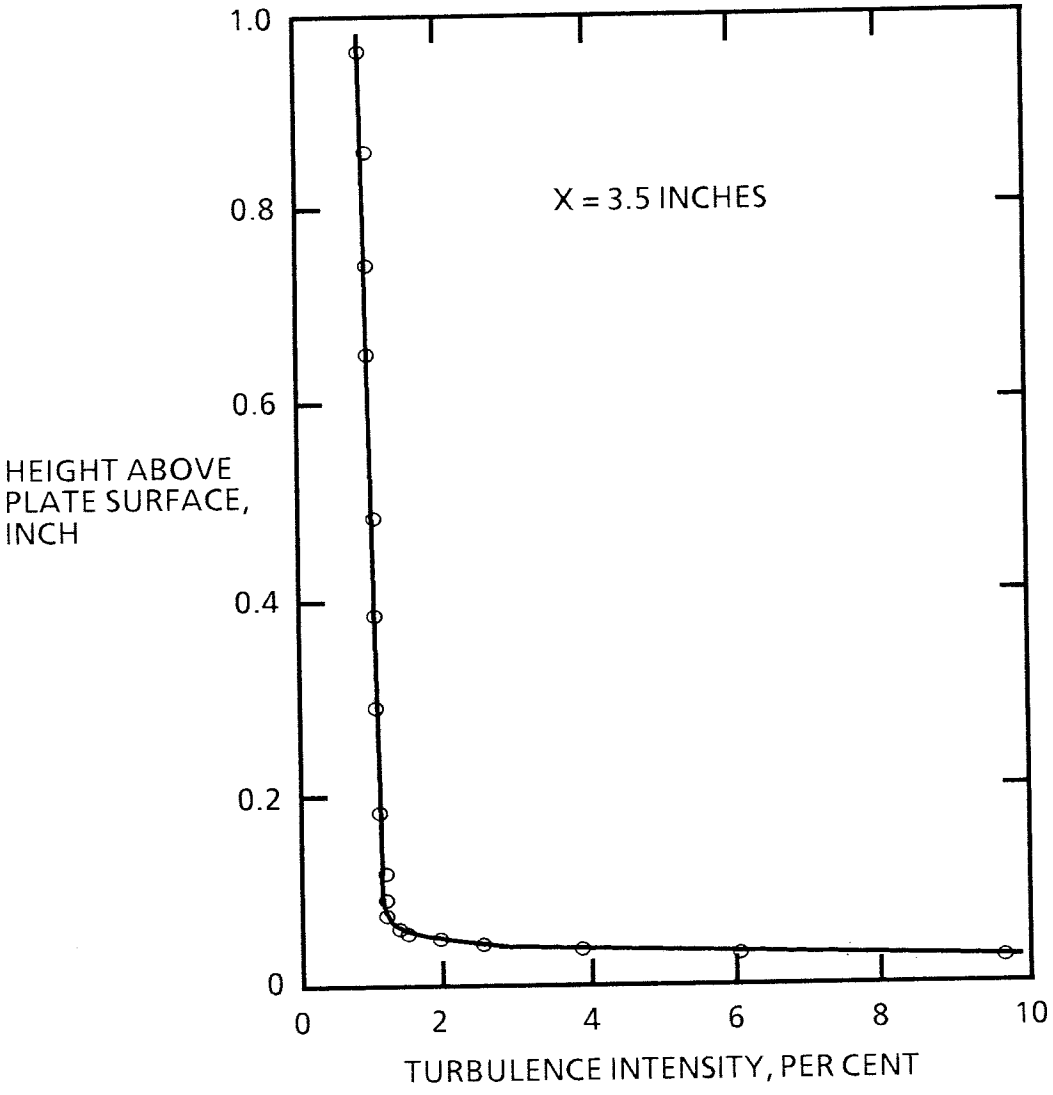

Figure 59 - Turbulence above test plate in configuration L